Available online at www.sciencedirect.com
ScienceDirect
Journal of Sound and Vibration 302 (2007) 806–820
JOURNAL OF SOUND AND VIBRATION
www.elsevier.com/locate/jsvi

Prediction methodology for ground vibration induced by passing trains on bridge structures

Yit-Jin Chen[a,*], Shen-Haw Ju[b], Sheng-Huoo Ni[b], Yi-Jiun Shen[c]

[a]*Department of Civil Engineering, Chung Yuan Christian University, Chung-Li 32023, Taiwan*
[b]*Department of Civil Engineering, National Cheng-Kung University, Tainan 70101, Taiwan*
[c]*China Engineering Consultants, Inc., 7F, 280, Chung-Hsiao E. Road, Section 4, Taipei 10694, Taiwan*

Received 15 March 2006; received in revised form 4 November 2006; accepted 6 December 2006
Available online 8 February 2007

Abstract

This study is a critical evaluation of the analysis method for ground vibration induced by passing trains on bridge structures. A wide variety of existing available evaluation methods and the influence factors are used for this evaluation. These primary influence factors include vibration source, ground vibration attenuation, and vibration receiver. In vibration source, a numerical model was developed to simulate the train system, train velocity, and bridge system, which is well comparable to the measurement results. For ground vibration attenuation, field measurement data are used for the back calculation of the attenuation coefficient (α) in terms of their geological conditions. The vibration receivers are also examined using a numerical model. Two prediction methods are presented for the evaluation of ground vibration induced by a train-bridge system. One is a hybrid method of numerical model, field measurement, and assessment handbook, while the other is a prediction method, which completely uses the numerical model for simulation.

1. Introduction

In recent decades, the train system which is built as elevated bridge structures has been widely used as a rapid transportation solution with the least environmental impact and requiring less space in a densely settled urban area. However, the ground vibration induced by the train system may cause disturbance and discomfort to the occupants. Experience shows that the building vibration induced by the train system can reach levels that cause human annoyance, possible damage to old and historical buildings, and interruption of sensitive instrumentation and processes. Therefore, ground vibration problems have drawn engineers' interest in recent years, and researchers have had the motivation to develop the prediction methodology for ground vibration induced by passing trains on bridge structures.

There are several existing vibration evaluation methods for preliminary vibration assessment in different countries. Among these, the US Department of Transportation developed manuals [1,2] to assess the vibration

*Corresponding author. Tel.: +886 3 2654227; fax: +886 3 2654299.
E-mail addresses: yjc@cycu.edu.tw (Y.-J. Chen), juju@mail.ncku.edu.tw (S.-H. Ju), tonyni@mail.ncku.edu.tw (S.-H. Ni), yjs@ceci.org.tw (Y.-J. Shen).

0022-460X/$ - see front matter © 2007 Elsevier Ltd. All rights reserved.
doi:10.1016/j.jsv.2006.12.010

impact for rapid transit and high-speed railways. In these manuals, factors affecting vibration source, vibration path, and vibration receiver are clearly specified. The designers can easily follow the manual to perform the preliminary design. The geological condition is known to have a significant effect on the vibration level; however, it is difficult to develop more than a broad-brush understanding of the vibration propagation characteristics on a general assessment stage. Much care must be taken when applying these manuals for areas with soft ground conditions. In addition, resonances of the building structure, particularly the floors, tend to counteract this attenuation and cause some amplification of the vibration. It is also difficult to estimate the effects of amplification from the general-purposed design manual.

In Japan, studies on train-induced vibration are mainly for Shinkansen, the name of a high-speed railway in Japan. The characteristics of cars related to ground vibration are car weight, number of cars, car length, wheelbase and bogie-center distance, and train speed. Reviewing the acceleration spectrum of 103 measurement sites, Yoshioka [3] interpreted the peak vibrations of these measurement results as the periodicity of axle arrangement and speed of train, as given below

$$f_1 = V/d_1, \quad f_2 = V/d_2, \quad \text{and} \quad f_3 = V/d_3, \tag{1}$$

where $f =$ peak frequencies; $V =$ train speed; $d_1 =$ distance of axles; $d_2 =$ distance of bogie-centre, and $d_3 =$ car length. The periodic effects of axle arrangement on different train speeds decide the peak frequency of the train-induced vibration spectrum. For the effects of elevated structures, Ejima [4] conducted a large-scale measurement for the issue of bridge structure sections, and the results indicated that the vibration value becomes smaller when the bending rigidity of the superstructure and concrete volume in the substructure of the bridge increase. For geological conditions, as examined in Ejima's data [4], Yoshioka [3] concluded that a bridge foundation built in soft ground may be easily agitated by vibration than one in hard ground.

For highly sensitive areas, detailed vibration prediction is usually essential when there is sufficient reason to suspect that adverse vibration impact and the general level of assessment are not suitable to the situation. The issue of bridge vibration due to moving vehicles has drawn attention since the 18th century, and two-dimensional (2-D) analyses were first conducted. Then a number of researchers investigated three-dimensional (3-D) models. Among these researches related to the 3-D analysis model, Kattis et al. [5] analyzed the problem of vibration isolation by trenches and a row of piles using the 3-D frequency domain boundary element method. Klein et al. [6] investigated a number of vibration isolation methods using the 3-D direct boundary element method. Ahmad et al. [7] used a 3-D boundary element algorithm incorporating quadratic elements to perform an extensive parametric study on the effectiveness of open trenches as wave barriers. Al-Hussaini and Ahmad [8] presented a numerical investigation of active isolation of machine foundations by in-filled trench wave barriers in 3-D half-space using the 3-D boundary element method. Dasgupta et al. [9] performed a 3-D boundary element analysis of the isolation of structures from ground-transmitted waves by open and in-filled trenches. Banerjee et al. [10] used the 3-D boundary element method to solve the problem of wave screening by barriers.

The numerical method involved in all of the above references is the boundary element method. The time-domain finite-element method (FEM) is seldom used to simulate the unbounded wave problem because the mesh profile requires a large number of degrees of freedom. Moreover, trainload is more complex than a point or line load, and thus the numerical simulation requires special considerations. Yang and Hung [11] employed the finite/infinite element to investigate the effectiveness of wave barriers in reducing the ground vibrations caused by the passage of trains. Ju and his researchers [12–14] established a 3-D time-domain FEM incorporating the absorbing boundary condition to simulate soil vibrations due to the moving train on the bridge system.

Therefore, to predict ground vibration due to the train system, existing methods in design manuals are not sufficient to reflect the complicated behavior. This paper thus provides a relatively simple and reasonable method for general situations. This method is originally from existing handbooks and design manuals, and is enhanced by field test results and improvement of modeling. For situations when a precise analysis is essential, a detailed prediction method is also proposed to perform and interpret the complicated vibration propagation. Both proposed prediction methods are supported by case examinations. However, the details for the theory of vibration propagation and numerical analysis are not discussed herein since the goal of this paper is for engineering application.

2. Proposed prediction methods for ground vibration

2.1. Simulation of vibration source

To perform detailed vibration impact assessment for a new planning line in the train system, the first step is to select a suitable model to represent the vibration source. Commonly, the ground vibration of most similar existing train lines was measured as the vibration source. However, the vehicle types (vehicle weight, train speed, axle distance, number of cars), supported bridge conditions (bridge type, bridge height, span, stiffness), and geological conditions for the sites of bridge structures are essential for obtaining similar vibration characteristics of the vibration sources. For engineering practice, there are no analytical methods of factoring out the effects of the above influence factors. This makes it very difficult to adjust the measurement results of currently operating rail lines to represent the vibration source of a newly planned rail line.

To overcome these situations, the numerical FEM model with absorbing boundary condition [14] is used to simulate the vibration source. First, the numerical model was established to simulate the vibration source, which is a bridge structure subjected to the train impact and transmitting the vibration wave through soil to some distances. Then the model was verified by comparing it with an in situ measurement of a currently operating rail line. This rail line was adopted as the major reference for the vibration assessment. Then the FEM model is used to revise the different conditions of bridge structures, number of cars, train speed, and soil conditions for the new planning line.

2.2. Simulation of ground vibration attenuation

Local geological conditions demonstrated a very large effect on the vibration level and the transmitting distances of ground vibration from the previous field measurement results [15–18]. Several wave propagation models have been developed in previous studies; however, many parameters need to be defined in the prediction models. The field measurement results of the investigated sites are used to represent the parameters of local geological conditions.

Ground vibration decay is primarily a function of soil damping and geometrical damping. Bornitz [19] considered both geometrical and material damping into an expression of R-wave attenuation as follows:

$$V_2 = V_1\sqrt{\frac{r_1}{r_2}}\mathrm{e}^{-\alpha(r_2-r_1)}, \tag{2}$$

where V_1 and V_2 are the vibration amplitudes of R-wave at distances r_1 and r_2, respectively, r_1 and r_2 are the distances from the vibration source, and α is the coefficient of attenuation for soil material. Previous research results presented the values of α depending on soil types and frequencies with a typical range from 0.001 to 0.08 m^{-1}. In this study, the vibration attenuation suggested by Bornitz is adopted to evaluate the effects of ground attenuation.

2.3. Simulation of vibration receiver

There are some handbooks for engineers to check the soil–structure coupling and building attenuation for the vibration receivers. The parameters for building conditions are foundation type, number of floors, and the damping ratio of the building. To estimate the vibration attenuation of soil–structure coupling, the suggested values in the design handbook [20] are used for the general design. As mentioned previously, the current handbooks are somewhat simple and rough, and they may be suitable for an initial estimation only.

For detailed vibration assessment, it is suggested that the numerical model be used to simulate the wave transmission within a building. The numerical simulation considers building stiffness, soil conditions, and natural frequencies of wave media. Moreover, the numerical simulation can predict the soil–building interaction, the attenuation within the building, and the resonance effects in some situations.

2.4. Scheme of proposed prediction methods

Combining the above simulations of vibration source, ground attenuation, and vibration receivers, two groups of prediction methods are suggested for the evaluation of ground vibration induced by a train system.

Table 1
Comparisons of two proposed prediction methods

Major analysis	Factor	Method 1	Method 2
Vibration source	Structure	Numerical model	Numerical model
	Train speed	Design manual [2]	Numerical model
	Geology	Measurement	Measurement and numerical model
Ground attenuation		Measurement	Measurement and numerical model
Vibration receiver		Design handbook [20]	Numerical model

The first method is a hybrid of field measurement, numerical model, and the current design handbook. The second method completely uses the numerical model for evaluation. Table 1 lists the comparisons of evaluation approach for the two proposed prediction methods. A brief description of the methods is discussed below.

Method 1: Method 1 is a combination of three easy approaches. It is simple and can be treated as a semi-empirical evaluation method. Method 1 is suitable for general preliminary analysis.

2.4.1. Vibration source

For vibration source, three adjustments are applied including the geological condition, bridge structure, and train velocity. Since the geological condition is one of the major factors for the characteristic of vibration level, a rail line (MRT Line 1) which has similar geological condition is selected to represent the vibration source of the new planning line (MRT Line 2). For the variation due to bridge structures, the numerical model is used to adjust the different vibration levels of these two different structure types. After the FEM model was successfully verified using the currently operating rail line (MRT Line 1), the new bridge structure model, which represents the new planning line (MRT Line 2) with the same geological condition, is established to adjust the vibration level. The difference of vibration levels between these two structure models is also considered in this prediction method.

For the factor of train speed, the relationship from the design manual of FTA [2] is used to calculate the adjustment of vibration level for the other speed, as given by

$$\text{adjustment VL (in dB)} = 20\log_{10}[V(\text{speed})/V(\text{speed}_{\text{ref}})], \tag{3}$$

where adjustment VL (in dB) = the adjustment of the vibration level of the train with the speed of V(speed), and $V(\text{speed}_{\text{ref}})$ = the train speed of the known vibration source. This adjustment cannot take into account the resonance effects of certain frequencies at the critical train speed due to periodic train-passing loading, as described previously [3].

2.4.2. Ground attenuation

The method in Section 2.2 is used in the evaluation of vibration attenuation. For simplification, the ground attenuation of Method 1 adopted the same coefficient of attenuation for every frequency.

2.4.3. Vibration receiver

The vibration attenuation of soil–structure coupling can refer to the design handbook [20]. The attenuation due to soil–foundation coupling loss in Method 1 is simplified to depend on the number of floors of the building.

Method 2: Method 2 is suitable for a detailed analysis, and a numerical model through vibration source to receiver is employed to evaluate the vibration level. First, the numerical model was established and examined using the bridge structure of the existing line (MRT Line 1) by the measurement results. Then the FEM model was modified according to the new structure type and geological condition of the new line (MRT Line 2).

3. Case examinations of the proposed methods

3.1. Measurement of vibration source

The measurement results of an operating train line (MRT Line 1) were used as the reference vibration source for the new planning line (MRT Line 2). The measuring equipment for this study includes a velocity transducer and a data acquisition system. Through an appropriate Fast Fourier Transform (FFT), the frequency response of the measurement is presented using a one-third-octave band for the central frequency range of 1–100 Hz. The ground vibration level is expressed in terms of its root-mean-square (rms) velocity using the decibel scale. The rms velocity level in decibels is defined as follows:

$$\mathrm{VL\,(in\ dB)} = 20\log_{10}\left(v_m/v_{\mathrm{ref}}\right), \tag{4}$$

in which v_{m} = the measured velocity and v_{ref} = the referred velocity $= 10^{-6}$ in/s $(= 2.54 \times 10^{-6}$ cm/s). Considering the structure types and geological conditions, one representative location was selected in this study for measurement. Ten passings of the transit train were measured, and the result was taken from the average of the 10 measurements.

The soil profile of this location mainly consists of soft clay (CL) with layers of fine sand (SP) or gravel (GP) embedded. The SPT-N values (standard penetration test) of the clay layer are less than 10, while the SPT-N values of the gravel layer are greater than 50. The span lengths of the steel bridge are 40–70–37 m. For the three-span continuous pre-stressed concrete (P.C.) bridge, the span lengths are all 23 m. The superstructure of the P.C. bridge is box girders with a depth of 1.4 m. The superstructure of the steel bridge is also box girders but with depths varying from 2.0 to 2.8 m. For the sub-structures, the diameter of the piers for the longest span (70 m) is 2.0 m, and the diameter of other piers is 1.6 m. The average height of the piers is 10 m. The pile foundation is adopted because of soft ground in this area. For the longer span of steel bridge, six piles are connected to a reinforced concrete pile cap, and four piles are used for other foundations. The diameters of piles were designed as 0.8–1.2 m and the pile lengths were 33–37 m. For the purpose of comparison, two bridge structure types on the same site are simultaneously measured as the transit car passes. One is for a steel bridge deck, while the other is for a concrete bridge.

The one-third octave bandwidth frequency responses for the steel bridge deck and the concrete bridge deck are shown in Figs. 1 and 2, respectively. The results measured at the steel bridge show that there are peak values at 3.15 Hz (48 dB), 5 Hz (55 dB), 6.3 Hz (58 dB) and 40 Hz (50 dB) in the X direction, while there are peak values at 1.25 Hz (50 dB), 1.6 Hz (50 dB), 6.3 Hz (56 dB), 12.5 Hz (60 dB), and 25 Hz (53 dB) in the Y direction. However, there are peak values at 1.6 Hz (60 dB), 2 Hz (59 dB), 5 Hz (70 dB), 6.3 Hz (73 dB), and 10 Hz (64 dB) in the Z direction. The largest velocity level is about 58 dB, 60 dB and 73 dB in the X, Y, and Z directions, respectively. The results measured at the concrete bridge show that there are peak values at 6.3 Hz (75 dB) and 63 Hz (72 dB) in the X direction, while there are peak values at 1.6 Hz (65 dB), 6.3 Hz (76 dB), 12.5 Hz (66 dB), 16 Hz (65 dB), 20 Hz (66 dB), 50 Hz (68 dB), and 63 Hz (69 dB) in the Y direction. However, there are peak values at 1.6 Hz (54 dB), 6.3 Hz (71 dB), 31.5 Hz (66 dB), and 40 Hz

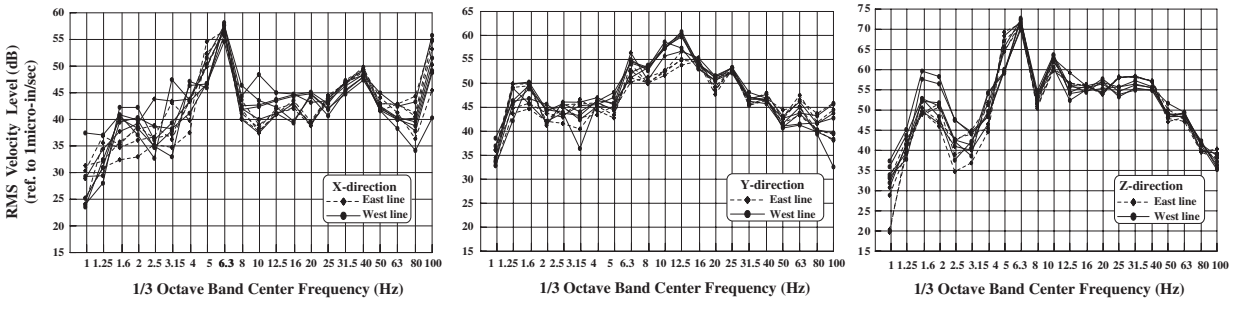

Fig. 1. One-third octave bandwidth frequency response of steel bridge.

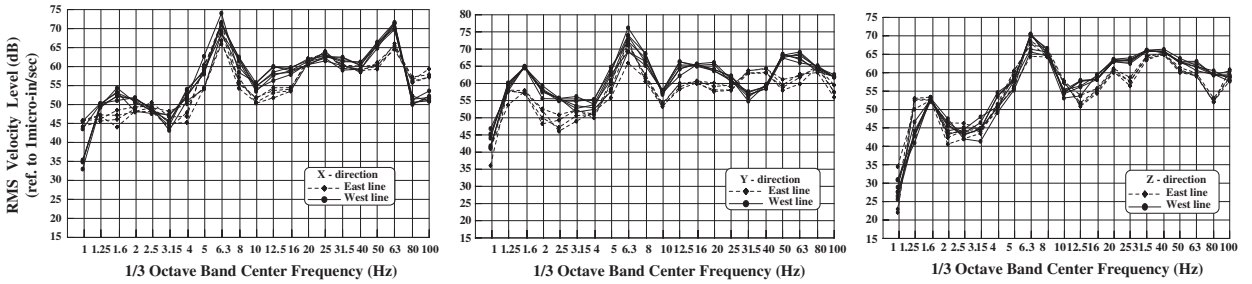

Fig. 2. One-third octave bandwidth frequency response of concrete bridge.

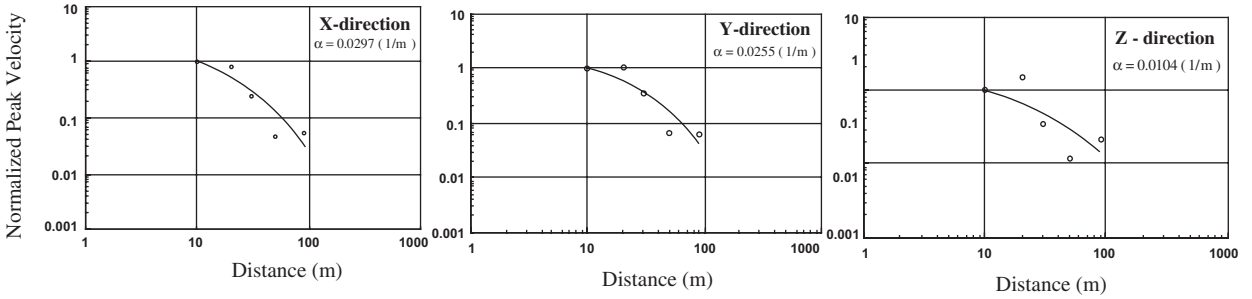

Fig. 3. α-attenuation coefficients from the back-analysis results.

(66 dB) in the Z direction. The largest velocity level is about 75 dB, 76 dB, and 71 dB in the X, Y, and Z directions, respectively.

3.2. Evaluation of vibration attenuation with distance

The vibration attenuations with distance for the new planning line (MRT Line 2) need to be evaluated. For the evaluation of α, a heavy hammer drop was used to generate the vibration source. The measured distance is about 100 m with six intervals and in a straight line. Then Eq. (2) was applied using the back-analysis procedure. The α attenuation coefficients are about 0.0297, 0.0255, and 0.0104 m^{-1}, respectively, for the x, y, and z directions, as shown in Fig. 3. These values look reasonable as compared with other recent experimental results [21]. The measurement results of Section 3.1 and the in situ test results in this section indicate that when the train supported by bridge structures is passing through the soft ground area, a low-frequency ground vibration exists, and the high level of vibration in low frequency is difficult to attenuate.

3.3. Analysis of the numerical model for operating train system [13]

The 3-D FEM incorporating the absorbing boundary condition was used to simulate soil vibration due to the moving train vehicle across the bridge. The simulation details and results are described below.

3.3.1. Absorbing boundary condition

For the spatial domain of $\{(x_1, x_2, x_3): x_1 > 0\}$, x_1 is the positive local direction points in the domain, while $x_1 = 0$ at the absorbing boundary, and u_i denotes the x_i-displacement. The first-order absorbing boundary condition is as follows:

$$\left(\frac{\partial}{\partial t} - c_i \frac{\partial}{\partial x_1}\right) u_i = 0 \quad \text{for } i = 1, 2, 3, \tag{5}$$

where c_i is the i-direction velocity divided by the cosine of the incidence angle. Ju and Wang [13] evaluated c_i using the square-root-of-the-sum-of-the-squares method as follows:

$$c_i = \sqrt{\left(\sum_{k=1}^{N} \frac{\partial u_{ik}}{\partial t}\frac{\partial u_{ik}}{\partial t}\right) \Big/ \left(\sum_{k=1}^{N} \frac{\partial u_{ik}}{\partial x_1}\frac{\partial u_{ik}}{\partial x_1}\right)} \quad \text{for} \quad i = 1, 2, 3, \tag{6}$$

where N is the number of nodes to obtain the average c_i. Then the forward Euler method derived from Eq. (5) is as follows:

$$u_{i,n+1} = u_{i,n} + \Delta t c_i \frac{\partial u_{i,n}}{\partial x_1}, \tag{7}$$

where $u_{i,n+1}$ is the i-direction displacement at the current time step, $u_{i,n}$ is the i-direction displacement at the last time step, and Δt is the time step length. In Eq. (7), all values at the right-hand side are given, so the current-controlled displacements are obtained. Thus, the time-history simulation of the infinite-domain wave can be achieved.

3.3.2. Moving wheel element

The train system was modeled as a number of moving wheels containing mass M_v, damping c_v and stiffness k_v, as shown in Fig. 4. The wheel element includes a wheel node and a number of target nodes. If the initial position and wheel velocity are known, the current position of the wheel node can be found. Afterward, the program finds the two target nodes in which the wheel node is located between them. If the two target nodes and the wheel node are set to nodes 1, 3, and 2, respectively, the mass, damping, and stiffness of the 3-node element can be calculated below using a similar procedure in the Ref. [14].

$$[S] = \begin{bmatrix} 0 & s_n \\ 1 & 0 \\ 0 & s_m \end{bmatrix} \begin{bmatrix} S_1 & S_2 \\ S_2 & S_3 \end{bmatrix} \begin{bmatrix} 0 & 1 & 0 \\ s_n & 0 & s_m \end{bmatrix} = \begin{bmatrix} s_n^2 S_3 & s_n S_2 & s_n s_m S_3 \\ s_n S_2 & S_1 & s_m S_2 \\ s_n s_m S_3 & s_m S_2 & s_m^2 S_3 \end{bmatrix}, \tag{8}$$

where $s_n = L_{2-3}/L_{1-3}$, L_{2-3} is the length between nodes 2 and 3, L_{1-3} is the length between nodes 1 and 3, $s_m = 1 - S_n$, and S_1, S_2, and S_3 obtained from the input data are the components of the mass, damping, or stiffness matrix of the vehicle wheel. For the mass, $S_1 = M_v$, $S_2 = 0$, and $S_3 = M_w$ (M_w is small and can be set to zero), for the damping $S_1 = S_3 = c_v$ and $S_2 = -c_v$, and for the stiffness $S_1 = S_3 = k_v$ and $S_2 = -k_v$, in which M_v, M_w, c_v and k_v are the train mass, wheel mass, damping, and stiffness, as shown in Fig. 3. $[S]$ is the 3-node mass, damping or stiffness matrix, which can be directly added to the global mass, damping or stiffness matrix. The direction of the 3-node matrix can be one of the three global translations or the three global rotations. To model the high-speed train, the target nodes passed by the train are first defined, and then each train wheel is modeled as a moving wheel element with appropriate velocity, initial position, load, mass, damping, and stiffness in global X, Y, and Z directions. Thus, a direct integration method can be used to perform the finite-element analysis.

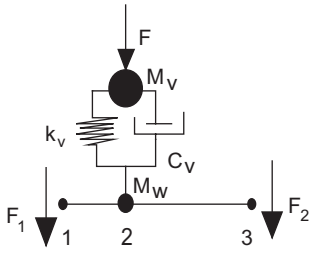

Fig. 4. Moving wheel element.

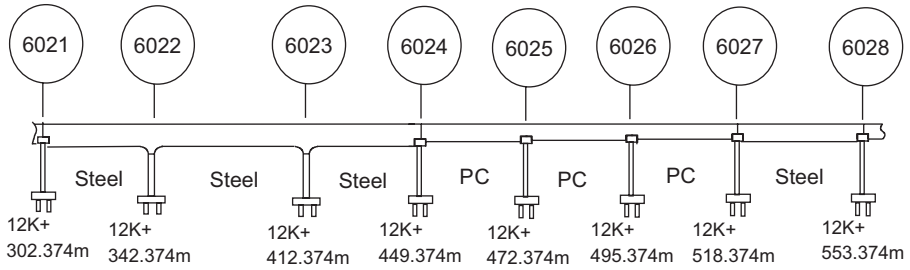

Fig. 5. Analyzed seven-bay bridge (four steel bays and three P.C. concrete bays).

Table 2
Soil conditions in FEM model

Depth (m)	V_P (m/s)	V_S (m/s)	G_d (kg/cm^2)	E_d (kg/cm^2)	K_d (kg/cm^2)	v_d
0–2	660	93	167	499	8221	0.489
2–4	857	93	167	501	14,015	0.494
4–8	857	143	417	1240	14,432	0.485
8–10	1580	143	417	1248	50,390	0.495
10–20	1580	278	1656	4915	51,286	0.484
20–22	1580	330	2333	6894	50,382	0.477

Note: V_p = P-wave velocity; V_s = shear wave velocity; G_d = soil dynamic shear modulus; E_d = soil dynamic Young's modulus; K_d = soil dynamic bulk modulus; v_d = soil dynamic Poisson's raio.

3.3.3. Illustration of bridge system

The analyzed bridge is located in MRT Line 1. The x-axis is the train moving direction, the y-axis is perpendicular to the train moving direction, and the negative z-axis is the soil depth direction. In this analysis model, the bridge system includes three spans of the P.C. bridge and four spans of steel bridge, as shown in Fig. 5. The span length and dimensions of the structure system are indicated in Section 3.1. The Young's modulus of the concrete is 3e7 kN/m^2 and that of the steel is 20.4e7 kN/m^2. The Poisson's ratio of the concrete is 0.15 and that of the steel is 0.3. The two factors of Rayleigh damping ([Damping] = δ[Mass] + β[Stiffness]) δ and β for the soil equal 0.4/s and 7.3e−4 s, respectively, which provides approximately 2% damping ratio at a frequency of 7 Hz. This damping was evaluated from the attenuation coefficients in Section 3.2. The two factors of Rayleigh damping, δ and β, for the bridge equal to 0.6/s and 5×10^{-4} s, respectively, which gives an approximately 2% damping ratio at a frequency of 12 Hz. This damping ratio is similar to that suggested for the steel or pre-stressed bridge from Ref. [22].

3.3.4. Finite-element model

The Newmark direct integration method with the consistent mass scheme was used in the finite-element model. Since the vibration induced by the MRT train is considerably small, the analysis is assumed to be linear elastic. The soil conditions in the analysis models are listed in Table 2, where only Young's modulus and Poisson's ratio of the soil were required in the linear Newmark finite-element analysis. The solution scheme was the SSOR preconditioned conjugated gradient method [23]. The finite-element model is 278 m long, 114 m wide, and 100 m deep, with the maximum square element size of $2 \times 2 \times 3$ m, in which the soil and bridge foundations were modeled by an eight-node 3-D solid element. The superstructure of the bridge was modeled by a two-node 3-D beam element, and the train system was modeled by the moving wheel elements. Five surfaces, except the top surface of the mesh, were modeled by the absorbing boundary condition to remove fake wave reflections, and the top surface was simulated as a free surface.

Fig. 6 shows the finite-element mesh. Within the area of the bridge piers along the soil surface, a master-slaved node scheme [24] was used to model the connection between the pier under ground (3-D solid element) and the pier above ground (3-D beam element). The master node was arranged at the pier center, and other

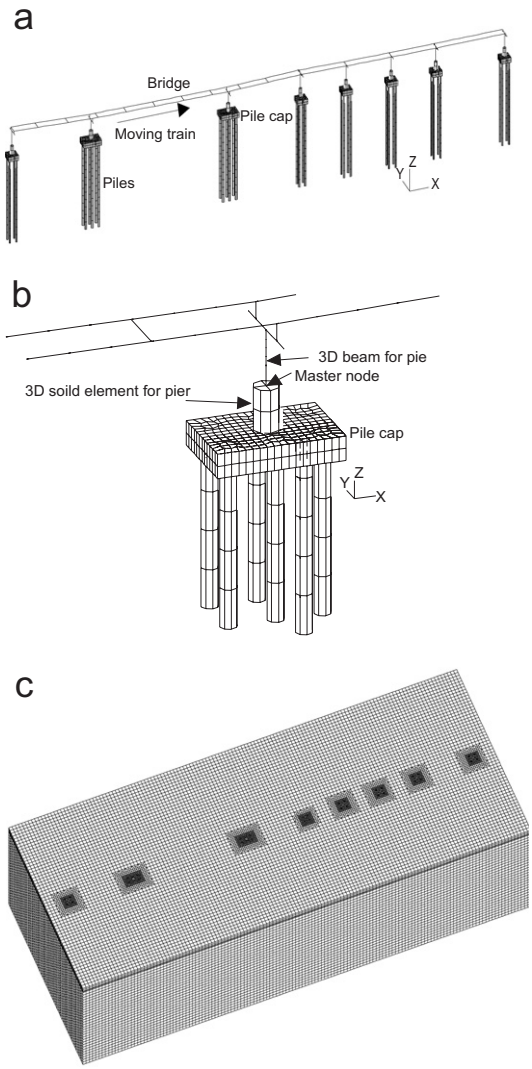

Fig. 6. Finite-element model. (a) Mesh of the superstructure and substructure except soils; (b) mesh adjacent to the pile cap and piles; (c) underground mesh.

nodes within this pier section on the soil surface were set to slaved nodes, whose three degrees of freedom are dominated by the 6-degree-of-freedom of the master node. Since each pier contains a master node, there are a total of eight master nodes in the finite-element mesh. The pile foundation including the pile caps and piles as mentioned in Section 3.1 was also modeled using the 8-node solid element. Figs. 6(a) and (b) show the finite-element mesh of the pile caps and piles, which are connected to the soil mesh as shown in Fig. 6(c). The Young's modulus and Poisson's ratio of the reinforced concrete pile foundation are 3e7 kN/m^2 and 0.15, respectively.

Fig. 6(c) shows a typical 3-D finite-element mesh, which contains 355,278 8-node brick elements, 297 3-D beam elements, 24 wheel elements in three global directions, and 71,697 absorbing boundaries. The time step length was set to 0.005 s, and 4096 time steps were simulated.

A 7-span bridge system modeled by 3-D beam elements as shown in Fig. 6a was adopted in this study. The superstructure of the bridge was divided into three groups using 3-D beam elements. The first group is the reinforced concrete bridge pier containing 96 elements. The second group is the box girders of the steel and the pre-stressed concrete bridge containing 164 elements. The third group is the connection parts

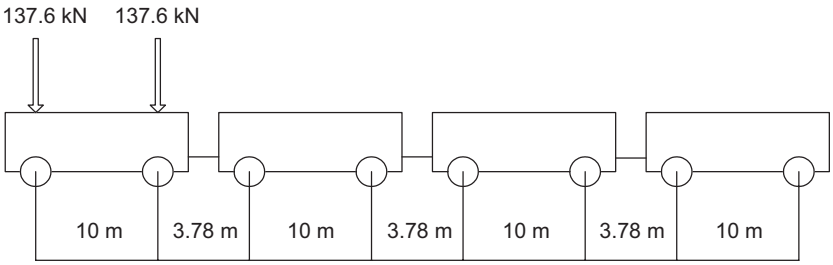

Fig. 7. Rapid transit system in MRT Line 1.

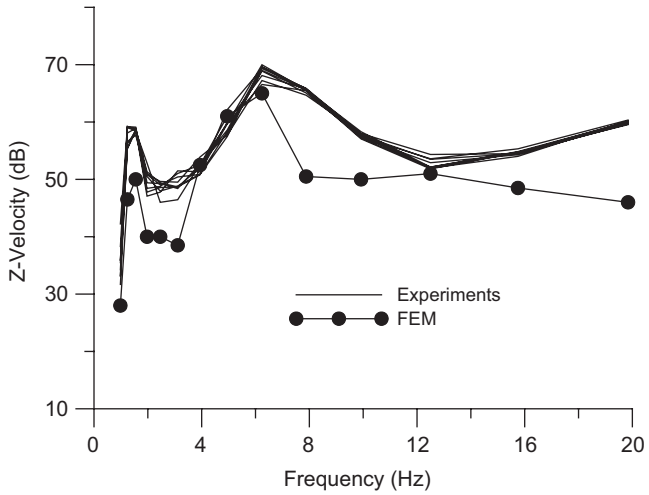

Fig. 8. Vertical velocity at pier 6025 on soil surface.

representing the eccentricity and the depth of pier caps and bridge girders, and the total number of these parts is 37 elements.

The train vehicles are shown in Fig. 7. There are four compartments and eight pairs of wheels in this system. The loading and compartment dimensions of this system are illustrated in Fig. 7. The vehicle velocity used in this analysis is 70 km/h.

3.3.5. Analysis results

Pier 6025 of MRT Line 1 bridge was used to measure the train-induced ground vibration velocity. The vibration transducers were placed on the soil surface just adjacent to the pier. Thus, the finite-element results of this research are compared with the experimental results. Fig. 8 shows the comparisons of the vertical velocity between finite element and experimental results for Pier 6025 (P.C. bridge). From Fig. 8, it can be seen that the differences of the results from the numerical model and site measurement are acceptable. The vibration peaks changing with frequencies from the finite-element analysis match well with those from the field experiments. It is noted that the field measurements contained ambient vibrations, and thus the vibrations computed by the finite-element analysis are a little lower than the measurement results in some frequencies.

3.4. Simulation of the numerical model for planning a train system

Based on above-examined numerical analytical model, the new model can be modified and developed to reflect the real situation of planning a train system. The trains in MRT Line 2 are similar to those in MRT Line 1 as shown in Fig. 7, except that the number of cars per train is increased to six. The analyzed bridge

Table 3
Five-story building in FEM model

Floor no.	Floor area $L \times W$ (m)	Floor height (m)	Column size $B \times d$ (m)	Beam size $B \times d$ (m)	Natural period (s) $T_B(x)$	Natural period (s) $T_B(y)$	Foundation beam size $B \times d$ (m)
5	45.8×12.6	3.0	0.6×0.6	0.4×0.6	0.5058	0.7134	0.6×1.0

Note: B = member width; d = member depth.

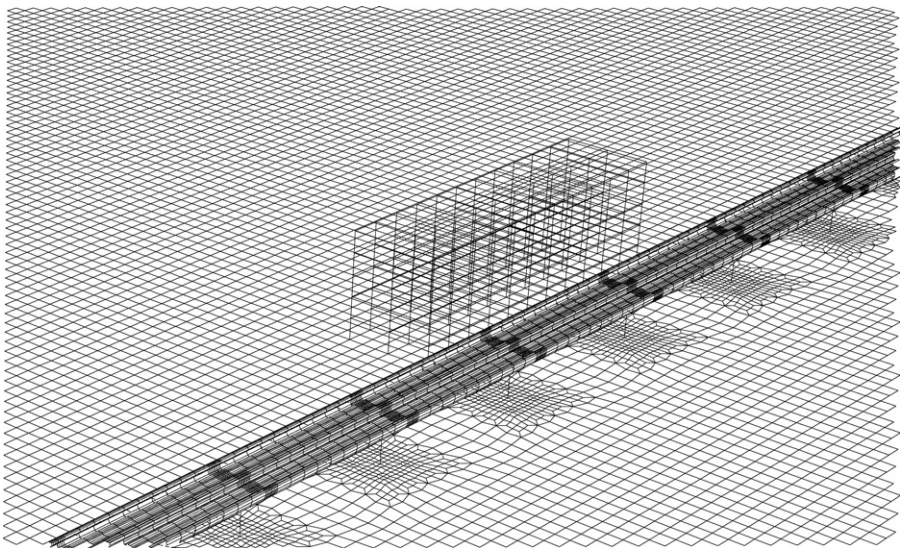

Fig. 9. Three-dimensional FEM model.

system includes 10 spans of the P.C. bridge with a span length of 25 m, and the cross-section of the superstructure in this analysis is a U-channel type. The soil conditions in the analysis models are listed in Table 2. A five-story reinforced concrete building with a mat foundation was adopted as the vibration receiver, and the distance from the track center to the edge of the building is 12.5 m. The dimensions of the building are 45.8 m by 12.6 m, where 12 by 3 columns are constructed. The neutral frequencies, floor dimensions, and member sizes of this building are listed in Table 3. The full 3-D finite-element model is shown in Fig. 9.

3.5. Case examination results of Method 1

Considering the structure types and geological conditions, the average measurement results of 10 passing trains in Fig. 2 are selected as the reference vibration source. However, the shape of the bridge structure and the train speed are adjusted according to Section 2.1. Since the bridge structure of MRT Line 1 is box type and that of MRT Line 2 is U type, the difference of ground vibration levels is corrected by FEM analysis, as shown in Fig. 10. The planned train speed in MRT Line 2 is 80 km/h, while the train speed in MRT Line 1 is 70 km/h. Eq. (3) is used as speed adjustment.

The vibration attenuation was measured according to Section 2.2, the suggested equation is shown in Eq. (2), and the results of vibration attenuation α coefficient in Section 3.2 were adopted. Since the vibration attenuation α coefficient is calculated only based on the overall vibration level, the same coefficient of attenuation is used for every frequency. The $r_1 = 1.0$ m, $r_2 = 12.5$ m are used since the vibration receiver is assumed to be 12.5 m from the track center. The vibration source was assumed to be a line source, and a set of train with six cars represented this line source. The vibration excited from each bridge pier within a train length is selected to represent the line source.

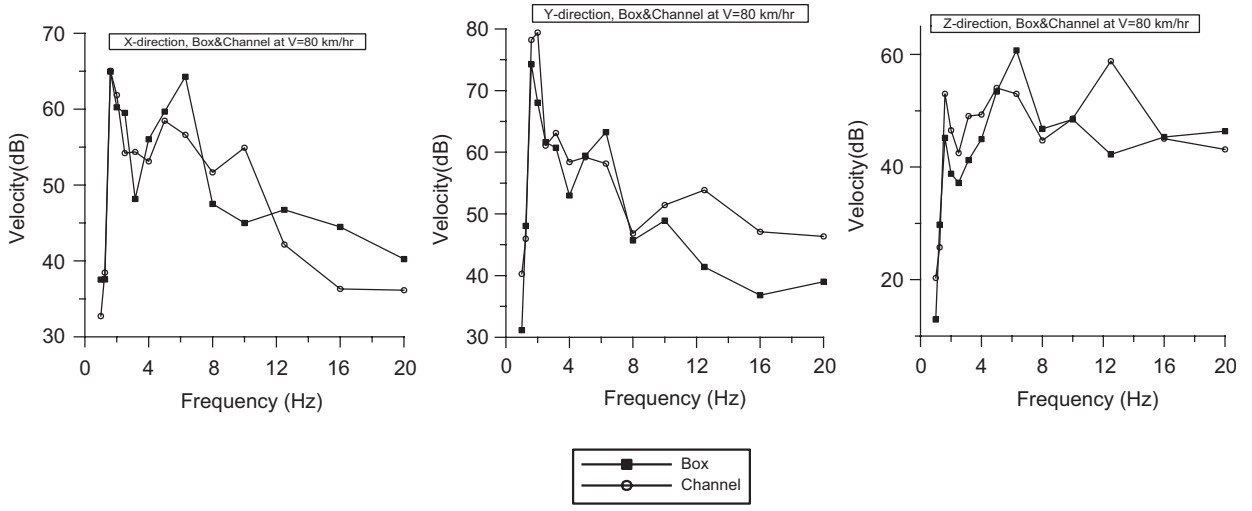

Fig. 10. Difference of vibration levels for box-type and U-type bridge structures.

Table 4
Vibration attenuation of soil–structure coupling [20]

Frequency (Hz)	4	8	16	32	63	125	250	500
Low rise building (dB)	−3	−5	−7	−8	−8	−7	−6	−4

Table 5
Building attenuation per floor [20]

Frequency (Hz)	4	8	16	32	63	125	250	500
Low rise building (dB)	0.4	0.4	0.8	1.0	1.4	2.0	2.4	3.0

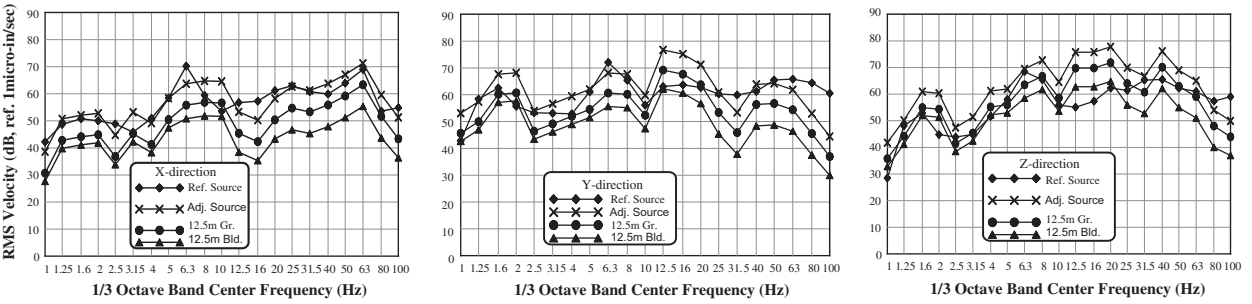

Fig. 11. Final results of estimated vibration level by Method 1 (80 km/h).

The five-story building was assumed to be the vibration receiver. According to Section 2.3, the attenuation of soil–structure coupling and building attenuation are calculated by the design handbook [20], as shown in Tables 4 and 5. The final results of estimated vibration levels by Method 1 are shown in Fig. 11. The "Ref. Source" represents the original reference source measured form MRT Line 1. The "Adj. Source" represents the vibration level after the adjustment of bridge structure and train speed, and the "12.5 m Gr." represents the calculated results of ground attenuation. It indicates the ground vibration level with the distance of 12.5 m from the track center, while the "12.5 m Bld." represents the estimated results of the five-story building. The

results of the overall vibration level in the X, Y, and Z directions, respectively, are 61, 68, and 71 dB. The design criteria in this residential area with more than 70 trains per day are 72 dB [2]. The assessment results satisfy the design criteria using Method 1.

The ground attenuation of Method 1 adopts the same coefficient of attenuation for every frequency, as shown in Fig. 11. However, the ground attenuation is varied for different frequencies based on a recent study [16]. The above-estimated results of ground attenuation can be further improved if the coefficients of attenuation are calculated for three types of frequency ranges, i.e. for low, middle, and high frequencies. In addition, the foundation types of building in Method 1 are classified just by the number of floors for evaluating the propagation loss of the vibration receiver. To simulate the attenuation due to soil–foundation coupling loss more precisely, further studies are needed to develop the relationships between building mass, natural frequency, foundation size, and the attenuation levels.

3.6. Case examination results of Method 2

A total of four speeds (between 60 and 90 km/h) were analyzed in the FEM model. Figs. 12 and 13 present the analysis results of vibration velocity (dB) of the five-story building for the train speeds of 70 and 80 km/h. It can be seen that the maximum velocity vibration levels of the bottom floor in the X, Y, and Z directions are 70, 72, and 71 dB, respectively, for the designed train speed 80 km/h, as shown in Fig. 12. However, if the train

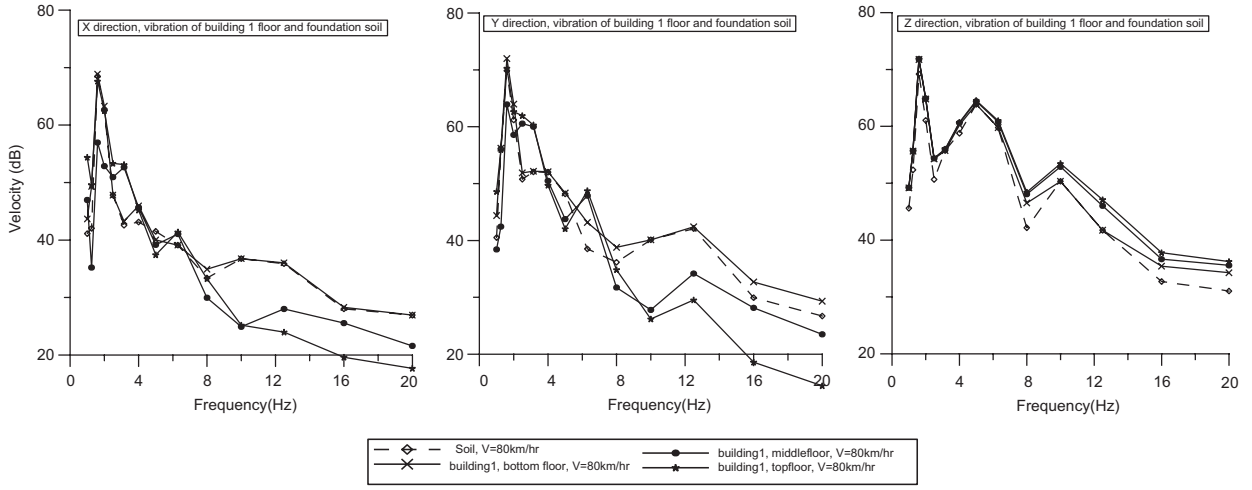

Fig. 12. Vibration levels of five-story building for the train speed of 80 km/h.

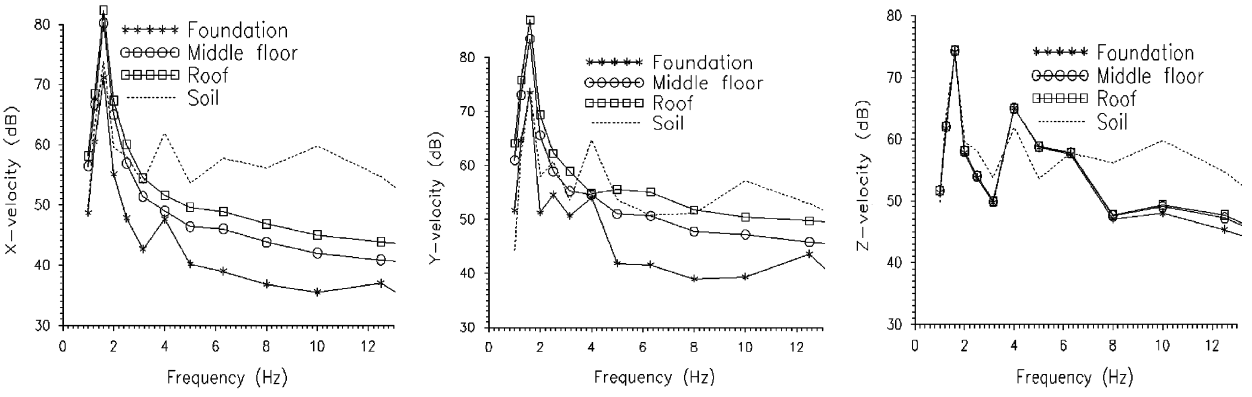

Fig. 13. Vibration levels of five-story building for the train speed of 70 km/h.

speed is decreased to 70 km/h, the maximum velocity vibration levels of the middle floor in the X, Y, and Z directions increase to 80, 83, and 74 dB for the frequency of 1.55 Hz, as shown in Fig. 13. The vibration levels become higher and can be attributed to the reason that the first train passing frequency is close to the first natural frequency of the building. When the MRT train is running with the speed of 70 km/h (or $V = 19.44$ m/s), it generates a train passing period $T_R = 0.7088$ s ($T_R = 1/f_R = L$ (car compartment length)/V_R(train speed) $= 13.78$ m/(19.44 m/s) $= 0.7088$ s for $n = 1$), which is close to the first natural frequency of the five-story building ($T_B(y) = 0.7134$ s) in the Y direction. The resonances of the building structure occur in the train speed of 70 km/h, and cause some amplification of the vibration. The amplification increases as the floor number increases. The results demonstrate that this method can predict the possibilities of resonances with the receiving building, the critical train speed, and the dominant frequency of the maximum vibration level. The existing design handbook usually neglects the possibilities of some amplification in low frequency.

4. Recommendations and conclusions

The existing available assessment methods were evaluated for ground vibration induced by a passing train in bridge structures with different bridge systems and geological conditions. Based on this evaluation, prediction methods were proposed, and conclusions were reached.

1. Proposed Method 1 is a semi-empirical evaluation method. The results of the case examination indicated that this method could be improved to simulate the vibration source and vibration path, which include too many uncertainties for the existing assessment method. This method can help engineers improve the accuracy of preliminary analysis, and is suitable to apply for a large number of preliminary assessments.
2. The ground attenuation of Method 1 adopts the same coefficient of attenuation for every frequency. Since the ground attenuation is varied for different frequencies, the estimated results of ground attenuation can be further improved if the coefficients of attenuation are calculated for three types of frequency ranges, i.e. low, middle, and high frequencies.
3. Since the foundation type of the building cannot be classified just by the number of floors, the attenuation due to soil–foundation coupling loss in Method 1 requires more studies to develop the relationships between building mass, natural frequency, foundation size, and the attenuation levels.
4. The proposed FEM solution of Method 2 provides a detailed prediction for ground vibration. This method is suitable for precise detailed assessments of highly sensitive areas. This solution can also predict the possibilities of resonances with the receiving building, the critical train speed, and the dominant frequency of the maximum vibration level. Therefore, this method is especially useful for cases when the vibration criteria are exceeded and vibration mitigation schemes are required.
5. When the train supported by the bridge structures passes through the soft ground area, a low-frequency ground vibration exists and is difficult to attenuate. Ground vibration prediction and mitigation need to take extra efforts in low-frequency vibration. However, the existing design handbook usually neglects the possibilities of some amplification in low frequency. Further modifications of the current design handbook are therefore essential in dealing with these amplification effects.

Acknowledgments

This study was supported by the National Science Council of ROC (Taiwan), under contract number: NSC 95-2221-E-033-011.

References

[1] US Department of Transportation Federal Railroad Administration (FRA), *Manual for High-speed Ground Transportation Noise and Vibration Impact Assessment*, 1998.

[2] US Department of Transportation Federal Transit Administration (FTA), *Manual for Transit Noise and Vibration Impact Assessment*, 1995.

[3] O. Yoshioka, Basic characteristics of Shinkansen-induced ground vibration and its reduction measures, *Proceedings of the International Workshop Wave 2000*, 2000, pp. 219–237.
[4] A. Ejima, Basic Research for Countermeasures against Ground Vibration from Concrete Girder Type Elevated of Shinkansen, Doctoral Thesis, University of Tokyo, 1980.
[5] S.E. Kattis, D. Polyzos, D.E. Beskos, Vibration isolation by a row of piles using a 3-d frequency domain BEM, *International Journal for Numerical Methods in Engineering* 46 (1999) 713–728.
[6] R. Klein, H. Antes, D. LeHouedec, Efficient 3D modelling of vibration isolation by open trenches, *Computers and Structures* 64 (1997) 809–817.
[7] S. Ahmad, T.M. Al-Hussaini, K.L. Fishman, Investigation on active isolation of machine foundations by open trenches, *Journal of Geotechnical Engineering, ASCE* 122 (1996) 454–461.
[8] T.M. Al-Hussaini, S. Ahmad, Active isolation of machine foundations by in-filled trench barriers, *Journal of Geotechnical Engineering, ASCE* 122 (1996) 288–294.
[9] B. Dasgupta, D.E. Beskos, I.G. Vardoulakis, Vibration isolation using open or fill trenches—part 2: 3-D homogeneous soil, *Computational Mechanics*, 6 (1990) 815–829.
[10] P.K. Banerjee, S. Ahmad, K. Chen, Advanced application of BEM to wave barriers in multi-layered three-dimensional soil media, *Earthquake Engineering and Structural Dynamics* 16 (1988) 1041–1060.
[11] Y.B. Yang, H.H. Hung, A parametric study of wave barriers for reduction of train-induced vibrations, *International Journal for Numerical Methods in Engineering* 40 (1997) 3729–3747.
[12] S.H. Ju, Finite element analyses of wave propagations due to high-speed train across bridges, *International Journal for Numerical Methods in Engineering* 54 (2002) 1391–1408.
[13] S.H. Ju, Y.M. Wang, Time-dependent absorbing boundary conditions for elastic wave propagation, *International Journal for Numerical Methods in Engineering* 50 (2001) 2159–2174.
[14] S.H. Ju, Y.J. Shen, P.J. Yen, Finite element analyses of wave propagations due to rapid transit system, *2002 WMSE Symposium Taipei*, 2002.
[15] Y.J. Shen, The application of deep foundations to mitigate ground vibration for a train-supporting viaduct structure in soft ground, *The International Deep Foundation Congress*, Vol. GSP 116, ASCE, New York, 2002, pp. 1098–1113.
[16] Y.J. Chen, S.H. Ni, Y.J. Shen, Evaluation of ground vibration induced by an urban train system, *The 10th IAEG International Congress*, Paper No. 773, 2006.
[17] S.H. Ni, C.W. Yang, Y.J. Shen, P.J. Yen, The characteristics of vibration induced by MRT-Mucha line rapid transit system, *2002 WMSE Symposium Taipei*, 2002.
[18] S.H. Ni, The experimental study of effectiveness of wave screening using trench (I): the vibration measurement and investigation of ground noise and related vibration parameters, Report for National Science Council, National Cheng-Kung University, 1999, pp. 38–72 (in Chinese).
[19] G. Bornitz, *Uber die Ausbreitung der von Groszkolbenmaschinen erzeugten Bodenschwingungen in die Tiefe*, J. Springer, Berlin, 1931.
[20] H.J. Saurenman, J.T. Nelson, G.P. Wilson, Handbook of Urban Rail and Noise Control, Report for US DOT/Transportation System Center, 1982.
[21] H. Xia, N. Zhang, Y.M. Cao, Experimental study of train-induced vibrations of environments and buildings, *Journal of Sound and Vibration* 280 (2005) 1017–1029.
[22] A.K. Chopra, *Dynamics of Structures: Theory and Applications to Earthquake Engineering*, second ed., Prentice-Hall, Englewood Cliffs, NJ, 1995 (p. 454, Table 11.2.1).
[23] S.H. Ju, K.S. Kung, Mass types, element orders and solving schemes for the Richards equation, *Computers and Geosciences* 23 (1997) 175–187.
[24] S.H. Ju, Investigating contact stresses on articular surfaces by 3-D rigid links, *Journal of Engineering Mechanics, ASCE* 123 (1997) 1253–1259.